Stress blunts serotonin- and hypocretin-evoked EPSCs in prefrontal cortex: Role of corticosterone-mediated apical dendritic atrophy

Rong-Jian Liu* and George K. Aghajanian

Department of Psychiatry, Yale University School of Medicine and Connecticut Mental Health Center, 34 Park Street, New Haven, CT 06508

Edited by Bruce S. McEwen, The Rockefeller University, New York, NY, and approved November 24, 2007 (received for review July 16, 2007)

Morphological studies show that repeated restraint stress leads to selective atrophy in the apical dendritic field of pyramidal cells in the medial prefrontal cortex (mPFC). However, the functional consequence of this selectivity remains unclear. The apical dendrite of layer V pyramidal neurons in the mPFC is a selective locus for the generation of increased excitatory postsynaptic currents (EPSCs) by serotonin (5-HT) and hypocretin (orexin). On that basis, we hypothesized that apical dendritic atrophy might result in a blunting of 5-HT- and hypocretin-induced excitatory responses. Using a combination of whole-cell recording and two-photon imaging in rat mPFC slices, we were able to correlate electrophysiological and morphological changes in the same layer V pyramidal neurons. Repeated mild restraint stress produced a decrement in both 5-HT- and hypocretin-induced EPSCs, an effect that was correlated with a decrease in apical tuft dendritic branch length and spine density in the distal tuft branches. Chronic treatment with the stress hormone corticosterone, while reducing 5-HT responses and generally mimicking the morphological effects of stress, failed to produce a significant decrease in hypocretin-induced EPSCs. Accentuating this difference, pretreatment of stressed animals with the glucocorticoid receptor antagonist RU486 blocked reductions in 5-HT-induced EPSCs but not hypocretin-induced EPSCs. We conclude: (*i*) stress-induced apical dendritic atrophy results in diminished responses to apically targeted excitatory inputs and (*ii*) corticosterone plays a greater role in stress-induced reductions in EPSCs evoked by 5-HT as compared with hypocretin, possibly reflecting the different pathways activated by the two transmitters.

two-photon imaging | apical tuft | slice | spine | rat

Stress induces neuronal atrophy in key limbic brain regions such as the hippocampus and medial prefrontal cortex (mPFC) that have been implicated in depressive illness (1). In layer II/III pyramidal neurons of the mPFC, repeated restraint stress has been shown to produce dendritic atrophy (2–5), an effect mimicked by high levels of corticosterone (6). Notably, these atrophic changes are restricted to the apical dendritic field. However, the functional implications at a cellular level of these localized effects of stress in the apical dendritic field are unclear. In a separate line of experiments in brain slices, we found that the apical dendrites are also the selective target of several stress–linked neurotransmitters/modulators, including serotonin (5-HT) and hypocretin/orexin, both of which induce a large increase in nonelectrically evoked ("spontaneous") excitatory postsynaptic currents (EPSCs) in layer V mPFC pyramidal cells in brain slices (7, 8). The effect of 5-HT is mediated by activation of 5-HT_{2A} receptors (7, 9), which are highly expressed on apical dendrites of layer V pyramidal neurons (10–13), and can be induced rapidly by the focal application of 5-HT to the apical but not basilar dendritic field in layer V pyramidal cells (7). Selective rescue of 5-HT_{2A} receptors in cortical pyramidal cells completely restores 5-HT-induced EPSCs that are lost in *5-HT2a*$^{-/-}$ mice, indicating that corticocortical rather than subcortical projections are involved (9). On the other hand, the effect of hypocretin is mediated via hypocretin 2 receptors located on the axonal terminals of ascending projections emanating from midline and intralaminar thalamocortical neurons, which selectively target spines on branches of apical dendrites of layer V pyramidal neurons (8). In any case, although different pathways are involved, both 5-HT and hypocretin-induced EPSCs are generated primarily in the apical dendritic field (7, 8).

The existence of 5-HT- and hypocretin-induced EPSC responses selective for the apical dendrite of layer V mPFC neurons creates an opportunity for investigating the possible effect of stress-induced apical dendritic atrophy on characterized excitatory inputs to the same dendritic subfield. In layer II/III pyramidal cells, 5-HT-induced EPSC responses are quite low (14) and hypocretin responses are virtually absent (8). Therefore, we focused on layer V pyramidal cells to permit a direct correlation between morphological and functional changes.

Here, we combined whole-cell patch clamp recording with two-photon imaging to determine whether 5-HT- and hypocretin-induced EPSCs are diminished by stress in association with dendritic atrophy in layer V pyramidal neurons. This approach allowed for direct correlations in the same cells between stress-induced morphological and functional changes occurring within a specific subfield of dendritic arborization.

Results

The Apical Tuft of Layer V Pyramidal Neurons in the Rat mPFC Is a Major Target for 5-HT- and Hypocretin-Induced EPSCs. Previous studies showed that 5-HT evoked more EPSCs when applied focally to the midapical rather than superficial regions of layer V pyramidal cell (7). However, in preliminary experiments, when the apical tuft was accidentally severed by the slicing procedure because of a surface trajectory of the apical dendritic shaft, there was an unexpectedly large reduction in EPSC responses to 5-HT. This observation led us to question whether the contribution of the apical tuft had been underestimated by previous studies because brief focal application of 5-HT would not have time to access deep portions of the tuft, which can extend hundreds of microns deep into the slice. To estimate more quantitatively the proportion of EPSCs derived from different parts of the apical dendrite, we compared responses to bath-applied 5-HT and hypocretin at near-maximal concentrations in eight pairs of neighboring cells, one with a surgical knife cut disconnecting the apical tuft near the bifurcation of the apical trunk and the other with its apical tuft left intact. Because the cut was quite distant

Author contributions: R.-J.L. and G.K.A. designed research; R.-J.L. performed research; R.-J.L. contributed new reagents/analytic tools; R.-J.L. analyzed data; and R.-J.L. and G.K.A. wrote the paper.

The authors declare no conflict of interest.

This article is a PNAS Direct Submission.

*To whom correspondence should be addressed. E-mail: rong-jian.liu@yale.edu.

This article contains supporting information online at www.pnas.org/cgi/content/full/0706679105/DC1.

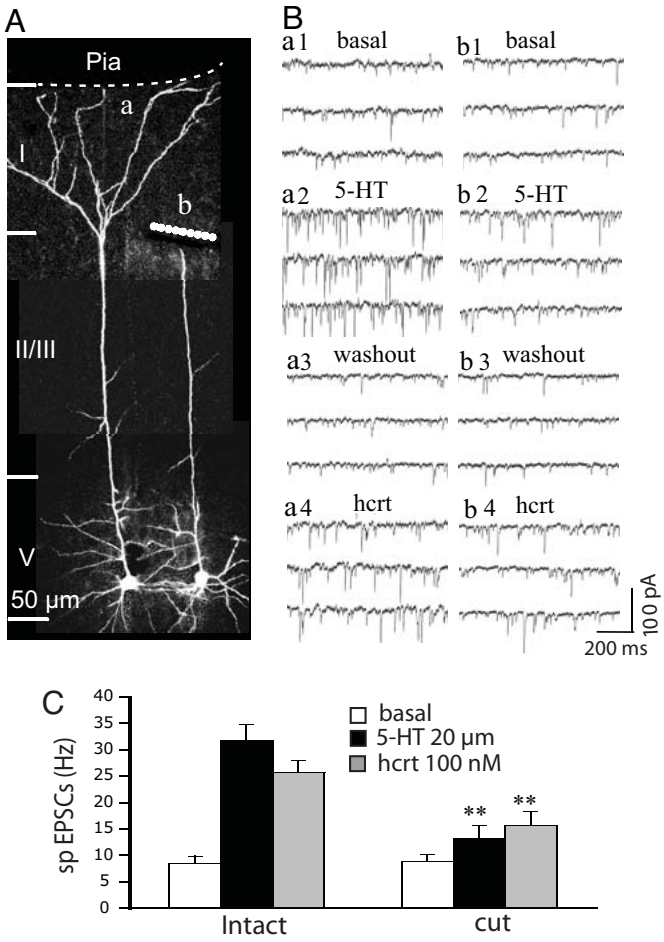

Fig. 1. 5-HT- and hypocretin-induced EPSCs are generated predominantly in the apical tufts of layer V pyramidal cells. (*A*) 3D Z-stack projections showing a pair of neighboring layer V pyramidal cells, one intact (a) and the other with its apical tuft detached (b). (*B*) Comparison of effects of 5-HT and hypocretin application on the EPSC response in these two cells; note that the cell with the detached apical tuft has a relatively low EPSC response to 5-HT and hypocretin (b1–4) compared with the intact cell (a1–4). (*C*) The mean EPSC frequency for eight pairs of cells shows that 5-HT-induced EPSCs are reduced by 80% and hypocretin-induced EPSCs are reduced by 60% in the group with detached apical tufts ($n = 8$; $P < 0.001$), confirming that a major proportion of EPSCs induced by 5-HT and hypocretin in layer V pyramidal cell in the mPFC are generated in the apical tuft. Note: dashed line depicts location of the pial membrane, which forms the medial border of mPFC; layers I–V are demarcated by horizontal lines.

from the site of recording (see Fig. 1*A*), basic electrophysiological properties recorded at the soma (e.g., resting membrane potential, spike amplitude, and input resistance) were not affected (data not shown). In the pairs shown in Fig. 1*A*, the intact cell (a) responded to bath-applied 5-HT with a marked increase in the frequency of EPSCs (Fig. 1*B*, a1 and a2); after washout of 5-HT, subsequent bath-applied hypocretin produced a similar increase in EPSCs (Fig. 1*B*, a3 and a4). In contrast, the cell with a severed apical tuft (cell b) had much lower responses to 5-HT and hypocretin. Fig. 1*C* gives mean data for the entire set of paired cells and shows an EPSC decrease of ≈80% for 5-HT (4.7 ± 2.6. vs. 23.3 ± 3.2 Hz; $n = 8$; $P < 0.001$) and ≈60% for hypocretin (6.8 ± 2.5 vs. 16.8 ± 2.3 Hz; $n = 8$; $P < 0.01$) in cells with a severed apical tuft as compared with controls. Note that basal frequency in the cut group was slightly higher than that in intact groups, but repeated-measures ANOVA analysis showed that the frequencies of EPSC between the cut and intact cell groups were not significantly different ($P > 0.05$). These results indicated that a majority of EPSCs induced by 5-HT and hypocretin are generated in the apical tuft, allowing us to focus on this well defined region of layer V pyramidal cells in subsequent experiments.

Total Apical Dendritic Branch Length and 5-HT- and Hypocretin-Induced EPSC Frequency Are Reduced After Repeated Immobilization Stress. In preliminary experiments, rats were subjected to 20 min of restraint stress for 3 or 7 days; in both cases, recordings were made 1 day after the last stress. Electrophysiological and morphological changes were seen after 7 but not 3 days of stress (data not shown). Therefore, in subsequent experiments only the 7-day stress protocol was used.

In both control and stressed groups, there was a broad morphological spectrum ranging from thin (simple) to thick (complex) tuft apical dendrites. In controls, whole-cell recording showed that thin tufted cells had low EPSC responses to 5-HT, whereas the thick tufted cells had high EPSC responses (Fig. 2*A*); the regression plot in Fig. 2*A Right* shows a high correlation between total apical tuft branch length and the frequency of 5-HT-induced EPSCs ($P < 0.0001$; $n = 35$). In the stress group, mean cell apical tuft branch length and 5-HT-induced EPSC frequency were both reduced (Fig. 2*C*). In addition, total oblique branch length was reduced, possibly contributing to the overall stress-induced decrement in EPSCs [supporting information (SI) Table 1]. Interestingly, the correlation between apical tuft length and EPSC frequency was lost after stress (Fig. 2*B*; $P > 0.05$; $n = 37$); this dissociation, which was most pronounced in some thick tufted cells (e.g., cell B4), implies that factors in addition to branch length are affecting EPSC responses. Hypocretin was also tested in ≈2/3 of the cells within each of the above groups and compared with 5-HT responses. As shown in Fig. 2*C*, cells in the stress group exhibited an overall reduction in apical tuft length (−24%; $P < 0.05$) and an even greater reduction in hypocretin-induced EPSC frequency (−46%; $P < 0.01$) than in 5-HT-induced EPSC frequency (−26%; $P < 0.05$). In addition, paired comparisons in control cells showed the frequencies of 5-HT- and hypocretin-induced EPSCs are highly correlated (SI Fig. 6*A*). Nevertheless, the selective 5-HT_{2A} antagonist MDL 100907 almost completely blocked 5-HT-induced EPSCs without affecting hypocretin-induced EPSCs (SI Fig. 6*B*).

Stress Induces a Decrease in Dendritic Spine Density and an Increase in Segmentation at Apical Tuft Dendritic Tips. In general agreement with the findings of Radley *et al.* (15), we found that stress significantly reduced the density of spines in distal ($P < 0.001$) and intermediate ($P < 0.001$) zones of the apical tuft, but did not affect the density of spines in more proximal regions (Fig. 3; $P > 0.05$; $n = 27$ cells for control, $n = 25$ cells for stress). Moreover, spine loss was often accompanied by an increase in segmentation or beading of distal segments, particularly at the tips of the tuft arbor as it extends to the pial membrane (Fig. 3*B1*; $P < 0.001$). However, even in the case of branch tips that showed extreme segmentation, more proximal branches could appear relatively normal (Fig. 3*B2*). As summarized in Fig. 3*C*, spine density was most dramatically reduced in the same distal regions that show segmentation. In contrast, the tips of oblique dendritic branches did not show this type of segmentation (SI Fig. 7). Segmentation may represent an early or transitional stage of branch tip disintegration, eventually leading to branch retraction.

Chronic Corticosterone Partially Mimics Stress. One possible mechanism for both stress-induced apical dendritic atrophy and reduction in EPSC responses would be corticosterone elevation secondary to hypothalamic-pituitary-adrenal axis activation (6, 15, 16). To test this possibility, a low dose of corticosterone was administered in the drinking water (100 μg/ml) for 7 days,

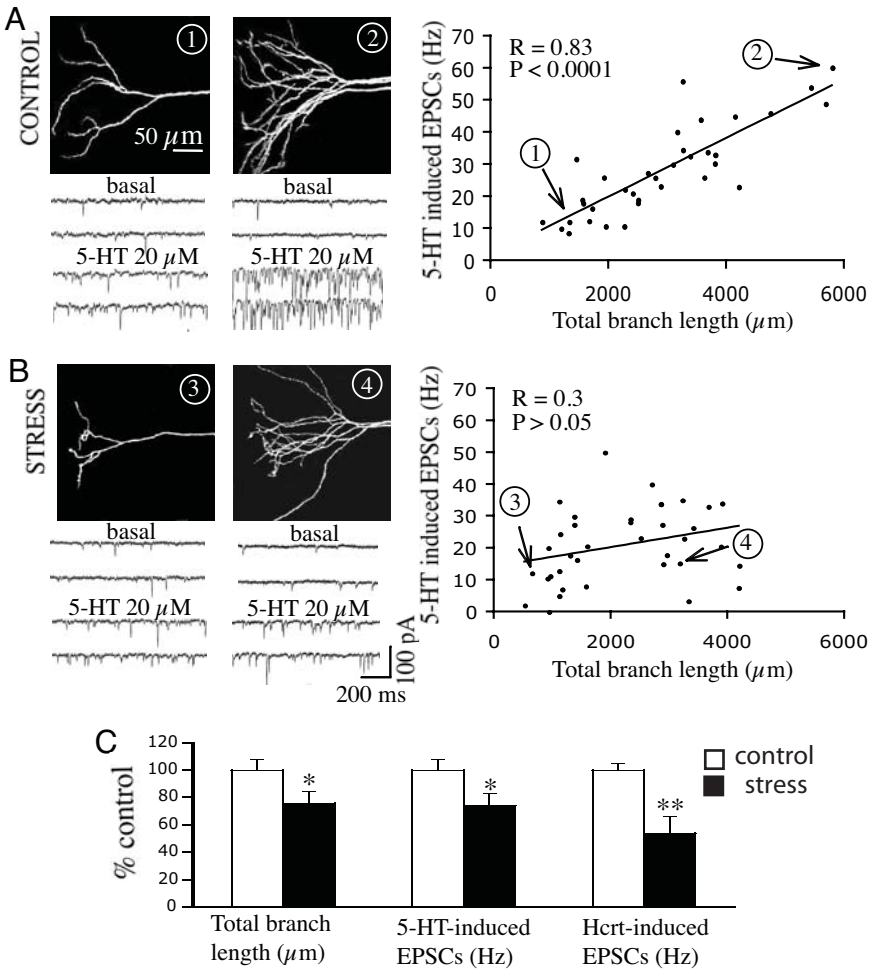

Fig. 2. Both the frequency of 5-HT- and hypocretin-induced EPSCs and total length of apical tuft branches are reduced in layer V pyramidal cells after repeated immobilization stress. (*A* and *B*) Projection images show two examples each of apical tufts in control (*A*) and chronic stress cells (*B*) (one thin tuft and one thick tuft). EPSC responses to 5-HT are shown below each image. Regression plot (*Upper Right*) in the control group shows a high correlation between the total length of apical tuft branches and the frequency of 5-HT-induced EPSCs; in the stress group this correlation is disrupted by greater variability and a disproportionate reduction in EPSC frequency at the upper end of the curve. Note the position of the four illustrated cells (1 to 4) on the regression plots are labeled by numbers and arrows. (*C*) Total apical tuft branch length and EPSCs induced by 5-HT and hypocretin are decreased in the same cells after chronic stress.

matching the duration of the stress protocol. Fig. 4*A* summarizes data comparing cells from control ($n = 23$) and corticosterone groups ($n = 34$). Total length of apical tuft branches was significantly reduced in corticosterone-treated rats (−27%) and was accompanied by a robust reduction in the frequency of 5-HT-induced EPSCs (−37%; $P < 0.01$). However, in the same cells there was only a borderline reduction in hypocretin-induced EPSCs (−23%; $P = 0.056$), opposite to the pattern seen after stress where the effect on hypocretin responses was greater than that of 5-HT. As with stress, corticosterone treatment led to a reduction in spine density and a marked increase in bead-like segments in the distal but not proximal portions of the apical tuft (Fig. 4*B*). However, the magnitude of reduction in spine density in the distal tuft branches was greater after stress than after corticosterone ($P = 0.008$); no differences were found in spine density in distal oblique branches between control, stress, and corticosterone groups (SI Fig. 7). These results suggest that although the overall effects of chronic stress and chronic corticosterone treatment are similar, the two treatments differ in the magnitude of changes they produce on EPSCs and spine density.

To evaluate further the role of corticosterone in mediating the effects of stress, the glucocorticoid receptor (GR) antagonist RU486 (10 mg/kg) was administered s.c. either 1 h before ($n = 6$) or 1 h after exposure ($n = 6$) to stress for each of 7 days, matching the duration of the stress-alone protocol. When RU486 was injected 1 h before stress, both the reduction of mean total apical tuft branch length and the frequency of 5-HT-induced EPSCs were prevented (Fig. 5*A*; $n = 17$ cells for control, $n = 18$ for vehicle + stress, $n = 17$ for RU + stress); no protection was found when RU486 was injected 1 h after stress (data not shown). In addition, prior RU486 treatment prevented a stress-induced reduction in spine density and segmentation in the distal portions of the apical tuft (Fig. 5*B*). However, RU486 provided no protection against the stress-induced decrease in the mean frequency of hypocretin-induced EPSCs. Together, these findings suggest that corticosterone elevation after stress may be responsible for overall dendritic atrophy and the reduction in 5-HT responses. However, factors in addition to corticosterone may be involved in impairing hypocretin responses.

Discussion

By a combination of whole-cell recording and two-photon imaging, we have shown in the same mPFC layer V pyramidal neurons that stress-induced dendritic atrophy is correlated with deficits in apically targeted excitatory responses. The most

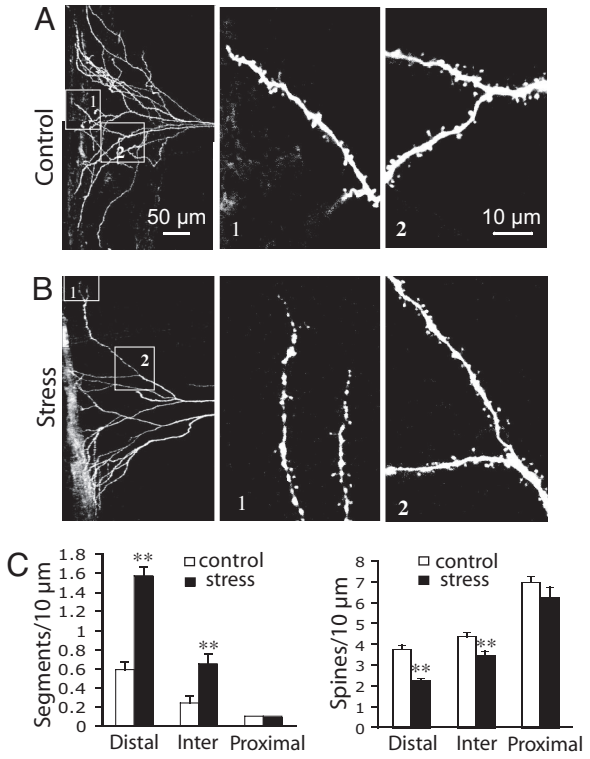

Fig. 3. Decrease in dendritic spine density and increase in segmentation/beading at apical tuft dendritic tips after chronic stress. (*A* and *B*) Z-stack projections showing the apical tuft for a layer V pyramidal cell in control (*A*) and stressed (*B*) groups. (*Insets*) At higher zoom branches at distal (no. 1) and intermediate (no. 2) zones are shown. Note the selective segmentation or beading of the distal tuft dendrites in the stressed group. (*C*) Bar graph comparing dendritic segmentation and spine density in distal, intermediate, and proximal zones in control and stressed groups. Note that stress increases segmentation and reduces spine density predominantly in distal ($P < 0.001$) and intermediate ($P < 0.001$) zones of the apical tuft.

profound atrophic changes occurred in the apical tuft, the same region where the majority of 5-HT and hypocretin-induced excitatory synaptic responses were found to originate. Interestingly, while mimicking many of the stress-induced morphological changes, corticosterone was much less effective than stress in altering EPSC responses to hypocretin, which targets the terminals of thalamocortical rather than corticocortical synapses. Accentuating these differences, the GR antagonist RU486 was found to block the reduction in 5-HT- but not hypocretin-induced EPSCs. These findings shed light on the mechanisms underlying different components of stress-related dendritic dysfunction.

Stress-Induced Selective Atrophy of Distal Apical Tuft Was Associated with an Increase in Segmentation or Beading. The finding of distal apical dendritic atrophy in layer V cells after repeated restraint stress confirms and extends earlier work performed in layer II/III cells (2–5). In addition, there was the observation of an increase in segmentation or beading, most strikingly in distal apical tuft branches as they approach the pial membrane. Although this type of morphological change has not been reported previously in relation to stress, it has been shown that acute exposure to the excitotoxin NMDA in hippocampal slices produces similar irregular dendritic swellings that occur preferentially in distal apical branches (17). Although it is uncertain whether the excitotoxin model can be used to explain our findings, it is interesting to note that acute restraint stress preferentially increases extracellular levels of glutamate in the mPFC as

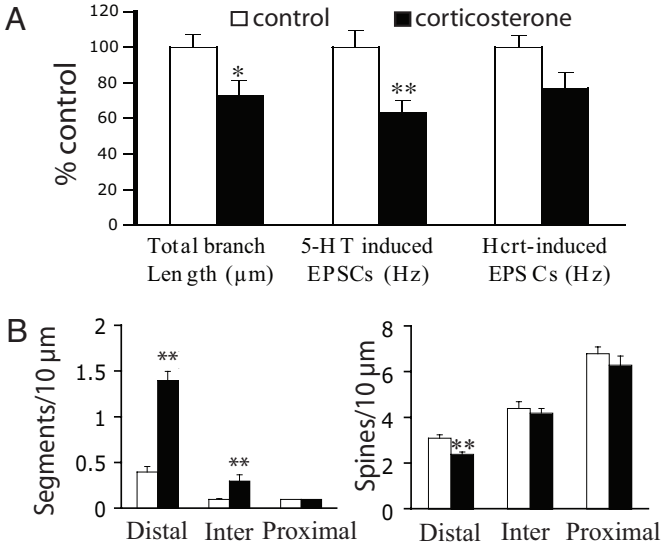

Fig. 4. Chronic administration of corticosterone (100 mg/ml in drinking water for 7 days) partially mimics the effects of stress. (*A*) Bar graphs comparing cells from control ($n = 32$, empty bar) and corticosterone ($n = 37$, filled bar) groups. As with stress exposure, the total length of apical tuft branches was significantly reduced in corticosterone-treated rats; the reduction was accompanied by a stronger decrease in the frequency of 5-HT-induced EPSCs and a slight decrease in the frequency of hypocretin-induced EPSCs (5-HT, − 37%; hypocretin, − 23%). (*B*) Mean data show that corticosterone treatment leads to a reduction in spine density associated with a marked increase in bead-like segmentation in the distal regions of the apical tufts.

compared with hippocampus (18), which may be a factor in the greater vulnerability of the mPFC to stress-induced dendritic damage.

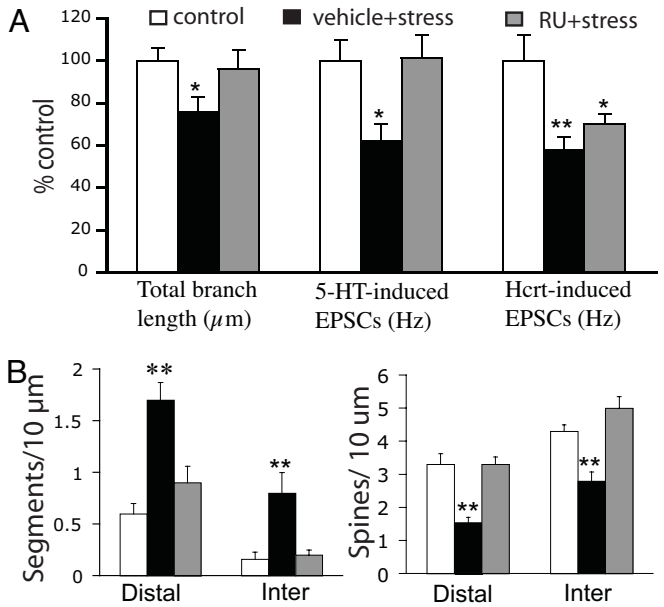

Fig. 5. Differential effects of the GR antagonist RU486 on stress-induced changes in 5-HT versus hypocretin responses. (*A*) Bar graphs show that GR antagonist RU486 prevents overall stress-induced morphological changes and the reduction of 5-HT- but not hypocretin-induced-EPSCs. (*B*) Bar graphs show the effect of RU486 on the stress-induced changes in spine density and segmentation. RU486 (10 mg/kg, s.c.) was injected 1 h before stress in the standard 7-day protocol. The data represent the mean ± SEM. *, $P < 0.05$; **, $P < 0.01$ versus control.

Characterization of Excitatory Inputs Affected by Chronic Stress. The apical dendritic synapses that are activated by hypocretin are innervated mainly by midline/intralaminar thalamic relay neurons, as shown by two-photon calcium imaging of single dendritic spines postsynaptic to anterogradely labeled thalamocortical terminals (8). The midline/intralaminar thalamic relay cells, which strongly express hypocretin2 receptors (19, 20) and receive inputs from hypothalamic hypocretin neurons, are directly depolarized by hypocretin (19). In contrast, direct depolarizing effects were not found in layer V pyramidal cell (8), consistent with the reported lack of hypocretin receptor 2 mRNA in layer V neurons of the cingulate cortex (20, 21). Another possible source of hypocretin-responsive inputs is subgriseal layer VII (VIb) (22), which sends a prominent projection to layer I (23). However, this pathway would not seem to be a major contributor to the EPSC response in layer V cells because the effect of hypocretin was almost totally eliminated by thalamic lesions (8).

Older literature with regard to the pathways mediating 5-HT induced EPSCs (24) conflicts with some more recent studies. The fact that selective rescue of 5-HT_{2A} receptors in cortical pyramidal cells of *htr2a*$^{-/-}$ mice totally restores 5-HT-induced EPSCs strongly suggests that 5-HT is acting primarily on corticortical pathways (9). As subcortical structures such as thalamus and basolateral amgdala that project to prefrontal cortex were devoid of 5-HT_{2A} receptors in the rescue mice (9), these subcortical inputs do not appear to play a primary role in mediating 5-HT_{2A}-induced responses. Although typical layer V pyramidal cells are not directly induced to fire by 5-HT beyond the first 2–3 weeks of postnatal development (25), it has been reported recently that 5-HT strongly depolarizes and initiates spiking activity in a special subpopulation of large "deep layer" pyramidal cells in the mPFC (26). These results suggest that recurrent collaterals from this deep layer subset rather than typical layer V pyramidal cells may be a source for the 5-HT-evoked EPSCs.

Corticosterone Partially Mimics the Effects of Stress both Electrophysiologically and Morphologically. Layer V pyramidal cells show atrophic changes similar to those seen previously in mPFC layer II/III pyramidal neurons after chronic treatment with corticosterone (6, 16). Despite this similarity, the electrophysiological changes after chronic corticosterone did not exactly mimic those induced by stress. Whereas stress produced a greater reduction of responses to hypocretin than 5-HT, the reverse was true after corticosterone. Furthermore, pretreatment of stressed animals with the GR antagonist RU486 blocked reductions in 5-HT- but not hypocretin-induced EPSCs. Thus, although both stress and corticosterone lead to apical dendritic atrophy and diminished EPSC responses to apically targeted excitatory inputs, corticosterone appears to play a greater role in stress-induced reductions in responses to 5-HT as compared with hypocretin. It is noteworthy that corticosterone also showed a smaller effect than stress on spine density in the distal apical tuft, suggesting that spine atrophy may not be indiscriminate but rather may have some degree of input specificity. Taken together, these differences indicate that the stress-induced hypocretin dysregulation may require the involvement of factors in addition to corticosterone. Indeed, the stress hormone corticotropin-releasing factor (CRF) directly activates hypocretin neurons, potentially mediating various aspects of the stress response (27). Moreover, the response to acute stress is severely impaired in CRF-R1 knockout mice (28). In general, these results are consistent with the idea that the full range of stress effects involves factors in addition to that of corticosterone (29, 30).

Behavioral and Clinical Implications. The midline/intralaminal thalamic projection to the mPFC is a critical link in the ascending arousal pathway. Hypocretin levels have been shown to correlate with states of attention and arousal and loss of hypocretin neurons results clinically in narcolepsy in humans (31). In rats, a low dose of hypocretin infused into the mPFC improves performance in a five-choice attention task (32). The reduction in hypocretin-activated synapses after stress suggests that a loss of thalamocortical inputs may contribute to the specific types of attention deficits that occur after repeated stress (33).

The ability of chronic corticosterone, at least in part, to mimic stress is of interest in relation to behavioral models of depression using mice that express different levels of GR. Heterozygous GR knockout mice ($GR^{+/-}$), with a 50% decrease in GR expression, exhibit normal baseline behaviors, but after stress exposure demonstrate increased learned helplessness associated with increased levels of endogenous corticosterone. These changes correlate with a down-regulation of brain-derived neurotrophic factor (BDNF) protein in $GR^{+/-}$ mice. Decreased expression of BDNF has also been found after the administration of exogenous corticosterone to normal rats (34). Interestingly, electrophysiological studies show that 5-HT-induced increases in EPSCs are reduced markedly in conditional BDNF knockout mice (35), suggesting a possible link between mechanism of stress-related dendritic atrophy and loss of 5-HT responses caused by corticosterone-induced BDNF deficiency.

Materials and Methods

Animals. Age-matched adult male albino rats (150–200 g; Harlan) were either exposed to a relatively mild stress or served as controls. Stressed rats were immobilized within a soft, flexible plastic cone with a breathing hole at the tip (DecapiCone; Braintree Scientific) for 20 min on 3 or 7 consecutive days. Then, a 1-day recovery period was allowed before animals were killed under chloral hydrate anesthesia, and mPFC slices were prepared. Paired stress and control rats were kept under routine laboratory housing conditions.

Brain Slice Preparation. Brain slices were prepared as described (36). Briefly, rats were anesthetized with chloral hydrate (400 mg/kg, i.p.), in adherence to protocols approved by the Yale Animal Care and Use Committee. After decapitation, the brains were removed rapidly and placed in ice-cold (≈4°C) artificial cerebrospinal fluid (ACSF) in which sucrose (252 mM) was substituted for NaCl (sucrose-ACSF) to prevent cell swelling. A block of tissue containing prefrontal cortex was dissected and coronal slices (400 μm) were cut in sucrose-ACSF with an oscillating-blade tissue slicer (Leica VT1000S). In some experiments, to evaluate the contribution of the apical tuft to EPSC responses, a surgical knife cut was made near the border of layer I and layer II. After placement of the slice in a submerged recording chamber, the bath temperature was raised to 32°C. Known concentrations of drugs dissolved in ACSF, applied through a stopcock arrangement at a fast flow rate (≈4 ml/min), reached the slice within 7–10 s. The standard ACSF (pH ≈7.35) was equilibrated with 95% O_2/5% CO_2 and contained 128 mM NaCl, 3 mM KCl, 2 mM $CaCl_2$, 2 mM $MgSO_4$, 24 mM $NaHCO_3$, 1.25 mM NaH_2PO_4, and 10 mM, D-glucose. A recovery period of ≈1–2 h was allowed before commencement of recording.

Electrophysiology. Pyramidal neurons in layer V were visualized by using an Olympus BX50WI microscope (×40 or ×60 IR lens) with infrared differential interference contrast (IR/DIC) videomicroscopy (Olympus), as described (8). Low-resistance patch pipettes (3–5 MΩ) were pulled from patch-clamp glass tubing (Warner Instruments) by using a Flaming-Brown Horizontal Puller (model P-97; Sutter Instruments). The pipettes were filled with the following solution: 115 mM K gluconate, 5 mM KCl, 2 mM $MgCl_2$, 2 mM Mg-ATP, 2 mM Na_2ATP, 10 mM Na_2-phosphocreatine, 0.4 mM Na_2GTP, and 10 mM Hepes, pH 7.33. Neurobiotin (0.3%) was added to the pipette solution to mark cells for later imaging. Pipettes were first tip-filled with regular patch solution before backfilling with the Neurobiotin solution to avoid ejecting excess dye into the extracellular space of the slice.

Whole-cell recordings were performed with an Axoclamp-2B amplifier (Axon Instruments). The output signal was low-pass-filtered at 3 KHz, amplified ×100 through Cyberamp, digitized at 15 kHz, and acquired by using pClamp 9.2/Digidata 1320 software (Axon Instruments). Series resistance, monitored throughout the experiment, was usually between 4 and 8 MΩ. To minimize series resistance errors, cells were discarded if series resistance rose above 10 Ω. Postsynaptic currents were studied in the continuous single-electrode voltage-clamp mode (3-kHz low-pass filter cutoff frequency); cells were usually clamped near their resting potential (≈75 mV ± 5 mV) to

minimize holding currents. After completion of recording, slices were transferred to 4% paraformaldehyde in 0.1 M phosphate buffer and stored overnight at 4°C. Slices were then processed with streptavidin conjugated to Alexa 594 (1/1,000; Invitrogen) for Neurobiotin visualization.

Imaging and Data Analysis. Labeled neurons within layer V of anterior cingulate (Cg1) and prelimbic mPFC (Cg3) were imaged with a two-photon laser scanning system. This consisted of a Ti:sapphire laser (Mai Tai; Spectra Physics) tuned to wavelength 810 nm and a direct detection Bio-Rad Radiance 2100 MP laser scanner (Zeiss Microimaging) mounted on an Olympus BX50WI microscope with ×40 (0.8 N.A.) or ×60 (0.9 N.A.) water-immersion objectives (Olympus). For analysis of total apical dendritic branch length, 3D Z-stacks were constructed from ≈40–250 sequential scans at low zoom (312 × 312 μm; ×40 lens) at 1-μm steps so as to include the entire apical tuft for a given cell within the slice. Total branch length was determined within the 3D matrix of each Z-stack by using Neurolucida 7 (MicroBrightField). For spine density analyses, Z-stacks consisting of 1–10 scans at high zoom (68 × 68 μm; ×60 lens) at 1-μm steps in the *z* axis were collected from the apical tuft arborization. Spine density and segmentation (beading) were analyzed in the X-Y plane of projection images by using Laser Sharp 2000 software (Bio-Rad). Spine density and segmentation (beading) were sampled in three zones: (*i*) tips of tuft branches as they approach the pial membrane; (*ii*) intermediate dendrites approximately midway between the pial membrane and bifurcation of apical trunk; and (*iii*) proximal tuft dendrites just distal to the bifurcation. Results were expressed in terms of total dendritic length, spine density, and segmentation density.

Drugs. 4-Pregnen-11β,21-diol-3,20-dione21-hemisuccinate (corticosterone hemisuccinate) was from Steraloids; 5-hydroxytryptamine creatinine sulfate (5-HT) and mifepristone (RU 486) were from Sigma; and hypocretin 2 (orexin B) was from American Peptide. All drug solutions were perfused at known concentrations through a stopcock assembly.

Analysis and Statistics. Electrophyiological data were displayed off-line with Clampfit software of pClamp 9.2 (Axon Instruments). Analysis of EPSCs from each 10-s block of (1 s) sweeps was performed with MiniAnalysis software (Synaptosoft). For statistical analysis, the total branch length was compared between groups by using Student's *t* test. The physiological data and the changes in spine density and bead-like segmentation were analyzed with repeated measures ANOVA, after a post hoc comparison. Values were represented as the mean ± SEM.

ACKNOWLEDGMENTS. This work was supported by National Institutes of Health Grant MH17871 and the state of Connecticut.

1. McEwen BS (2005) *Metabolism* 54:20–23.
2. Cook SC, Wellman CL (2004) *J Neurobiol* 60:236–248.
3. Radley JJ, Sisti HM, Hao J, Rocher AB, McCall T, Hof PR, McEwen BS, Morrison JH (2004) *Neuroscience* 125:1–6.
4. Brown SM, Henning S, Wellman CL (2005) *Cereb Cortex* 15:1714–1722.
5. Izquierdo A, Wellman CL, Holmes A (2006) *J Neurosci* 26:5733–5738.
6. Wellman CL (2001) *J Neurobiol* 49:245–253.
7. Aghajanian GK, Marek GJ (1997) *Neuropharmacology* 36:589–599.
8. Lambe EK, Aghajanian GK (2003) *Neuron* 40:139–150.
9. Weisstaub NV, Zhou M, Lira A, Lambe E, Gonzalez-Maeso J, Hornung JP, Sibille E, Underwood M, Itohara S, Dauer WT, *et al.* (2006) *Science* 313:536–540.
10. Willins DL, Deutch AY, Roth BL (1997) *Synapse* 27:79–82.
11. Jakab RL, Goldman-Rakic PS (1998) *Proc Natl Acad Sci USA* 95:735–740.
12. Cornea-Hebert V, Riad M, Wu C, Singh SK, Descarries L (1999) *J Comp Neurol* 409:187–209.
13. Miner LA, Backstrom JR, Sanders-Bush E, Sesack SR (2003) *Neuroscience* 116:107–117.
14. Lambe EK, Goldman-Rakic PS, Aghajanian GK (2000) *Cereb Cortex* 10:974–980.
15. Radley JJ, Rocher AB, Miller M, Janssen WG, Liston C, Hof PR, McEwen BS, Morrison JH (2006) *Cereb Cortex* 16:313–320.
16. Cerqueira JJ, Taipa R, Uylings HB, Almeida OF, Sousa N (2007) *Cereb Cortex* 17:1998–2006.
17. Hoskison MM, Yanagawa Y, Obata K, Shuttleworth CW (2007) *Neuroscience* 145:66–79.
18. Moghaddam B (1993) *J Neurochem* 60:1650–1657.
19. Bayer L, Eggermann E, Saint-Mleux B, Machard D, Jones BE, Muhlethaler M, Serafin M (2002) *J Neurosci* 22:7835–7839.
20. Marcus JN, Aschkenasi CJ, Lee CE, Chemelli RM, Saper CB, Yanagisawa M, Elmquist JK (2001) *J Comp Neurol* 435:6–25.
21. Trivedi P, Yu H, MacNeil DJ, Van der Ploeg LH, Guan XM (1998) *FEBS Lett* 438:71–75.
22. Bayer L, Serafin M, Eggermann E, Saint-Mleux B, Machard D, Jones BE, Muhlethaler M (2004) *J Neurosci* 24:6760–6764.
23. Clancy B, Cauller LJ (1999) *J Comp Neurol* 407:275–286.
24. Marek GJ, Wright RA, Gewirtz JC, Schoepp DD (2001) *Neuroscience* 105:379–392.
25. Zhang ZW (2003) *J Neurosci* 23:3373–3384.
26. Beique JC, Imad M, Mladenovic L, Gingrich JA, Andrade R (2007) *Proc Natl Acad Sci USA* 104:9870–9875.
27. Winsky-Sommerer R, Yamanaka A, Diano S, Borok E, Roberts AJ, Sakurai T, Kilduff TS, Horvath TL, de Lecea L (2004) *J Neurosci* 24:11439–11448.
28. Paneda C, Winsky-Sommerer R, Boutrel B, de Lecea L (2005) *Drug News Perspect* 18:250–255.
29. Nacher J, Pham K, Gil-Fernandez V, McEwen BS (2004) *Neuroscience* 126:503–509.
30. McEwen BS (1999) *Annu Rev Neurosci* 22:105–122.
31. Sutcliffe JG, de Lecea L (2002) *Nat Rev Neurosci* 3:339–349.
32. Lambe EK, Olausson P, Horst NK, Taylor JR, Aghajanian GK (2005) *J Neurosci* 25:5225–5229.
33. Liston C, Miller MM, Goldwater DS, Radley JJ, Rocher AB, Hof PR, Morrison JH, McEwen BS (2006) *J Neurosci* 26:7870–7874.
34. Ridder S, Chourbaji S, Hellweg R, Urani A, Zacher C, Schmid W, Zink M, Hortnagl H, Flor H, Henn FA, *et al.* (2005) *J Neurosci* 25:6243–6250.
35. Rios M, Lambe EK, Liu R, Teillon S, Liu J, Akbarian S, Roffler-Tarlov S, Jaenisch R, Aghajanian GK (2006) *J Neurobiol* 66:408–420.
36. Liu RJ, van den Pol AN, Aghajanian GK (2002) *J Neurosci* 22:9453–9464.